Hindawi Publishing Corporation
International Journal of Photoenergy
Volume 2015, Article ID 478978, 7 pages
http://dx.doi.org/10.1155/2015/478978

Research Article

Prediction of a New Phase of Cu_xS near Stoichiometric Composition

Prashant Khatri and Muhammad N. Huda

Department of Physics, University of Texas at Arlington, Arlington, TX 76019, USA

Correspondence should be addressed to Muhammad N. Huda; huda@uta.edu

Received 16 November 2014; Revised 15 January 2015; Accepted 3 March 2015

Academic Editor: Mahmoud M. El-Nahass

Copyright © 2015 P. Khatri and M. N. Huda. This is an open access article distributed under the Creative Commons Attribution License, which permits unrestricted use, distribution, and reproduction in any medium, provided the original work is properly cited.

Cu_2S is known to be a promising solar absorber material due to its suitable band gap and the abundance of its constituent elements. Cu_2S is known to have complex phase structures depending on the concentration of Cu vacancies. Its instability of phases is due to favorable formation of Cu vacancies and the mobility of Cu atoms within the crystal. Understanding its phase structures is of crucial important for its application as solar absorber material. In this paper, we have predicted a new crystal phase of copper sulfide (Cu_xS) around chemical composition of $x = 1.98$ by utilizing crystal database search and density functional theory. We have shown that this new crystal phase of Cu_xS is more favorable than low chalcocite structure even at stoichiometric composition of $x = 2$. However, Cu vacancy formation probability was found to be higher in this new phase than the low chalcocite structure.

1. Introduction

Cu_2S is a well-known semiconductor which has the potential to play an important role as a solar absorber material. Thin films of heterojunctions such as Cu_2S/CdS have shown an efficiency of 9-10% in the past [1–4]. However, Cu_2S shows complex structural behavior. Experimental results so far have shown that stoichiometric Cu_2S mainly exists in three forms: monoclinic phase (low chalcocite) forms at temperature below 104°C, hexagonal phase (high chalcocite) forms between 104 and 436°C, and cubic phase forms at temperature 436°C or higher [5, 6]. Theoretical calculations on three chalcocites have shown consistency with experimental facts revealing low chalcocite is favorable at 0 K [7, 8]. The low chalcocite has 96 Cu and 48 S atoms and is monoclinic in nature. A major problem in Cu_2S is the copper atom's instability towards the formation of copper vacancies; this leads to the formation of different crystal structures depending on Cu vacancy concentrations [7–12]. In addition, this formation of high copper vacancies results in very high p-type doping [13] causing the material to behave like a degenerate semiconductor. Moreover, in Cu_2S, the positions of Cu within the sublattice of S atoms are not well defined [7, 8] as copper atoms are mobile in nature in Cu_2S [14, 15]. Despite being earth abundant and nontoxic, these problems hindered the further study of Cu_2S in photovoltaic community for some time.

Table 1 provides names of known Cu_2S phases those that are experimentally identified with their composition. Experimentally observed band gaps of these Cu_xS phases fall in the range of 1.1–1.2 eV; however, the nature of these band gaps is not well identified yet [7, 8]. Various studies have stated that studying and understanding Cu_xS have been a long term challenge [4–6, 16–18], especially in computational works, which is mainly due to the complex behavior of copper in Cu_2S. Experimental and theoretical studies have shown that Cu vacancies are inevitable in Cu_2S. Hence, for the effective usage as a solar absorber material an understanding and a detail map of Cu_2S phases based on Cu vacancy concentrations are essential. To avoid excessive p-type doping, it is desirable to stabilize a phase of Cu_xS near $x = 2$. It can be assumed that at thermodynamic equilibrium, low chalcocite structure may sustain these composition ranges near $x = 2$. However, this has not been tested and not reported anywhere. To the best of our knowledge, no phases have been so far identified with the chemical composition $2 > x > 1.97$. Hence, it is important to study Cu_xS compounds with different possible structures with a value of x

Table 1: Names of different phases of Cu_xS with respect to x are shown.

x	Name
2	Chalcocite [5, 6]
1.94	Djurleite [6]
1.8	Digenite [19]
1.75	Anilite [20]

near 2 to find a possible strategy to stabilize such phase. Furthermore, it is possible that the ambiguity of Cu positions in crystals may also be due to the coexistence of more than one crystal phase which are energetically close to each other. Hence, identification of thermodynamically stable new structures will shed light on this problem. Stabilization of such structures may lead to a new route for Cu_xS as stable solar absorber materials. In this paper, by using crystal database and density functional theory (DFT) based total energy calculations, we predicted a new stable phase for $Cu_{x\approx1.98}S$, which has not been reported before.

2. Computational Methodology

Density functional theory (DFT) as implemented in *Vienna Ab-initio Simulation Package* (VASP) [21, 22] has been used for calculating the total energy of different possible Cu_2S/Cu_xS phases. In our calculation, the generalized gradient approximation (GGA) functional known as Perdew-Burke-Ernzerhof (PBE) [23] has been used with the projected augmented wave (PAW) [24, 25] method. For ionic relaxation, each ion was relaxed until the force on it is equal or less than 0.01 eV/Å, and 400 eV was used for the energy cut-off for the plane wave basis set. It is well known that DFT usually underestimates band gaps; especially for some phases of Cu_2S it gives negative band gap. A computationally economical way to correct such problem is to invoke DFT + U method, which not only opens the band gap, but also tends to provide a d^{10} configuration for Cu in Cu_2S. Hence, we also calculated electronic properties, such as band gaps, of Cu_xS with DFT + U [26, 27] with $U = 7$ eV and $J = 1$ eV which provides an effective U ($= U - J$) of 6 eV. In DFT + U the extra term U is a Hubbard-like potential added to the Kohn-Sham DFT Hamiltonian. This provides extra correlation to an orbital by introducing intraband repulsive interaction, which results in a relatively more localized band. For 3D transition metals this method has been proven to be very effective. Justification for choosing this value will be discussed in the following section.

As we are searching for a stable phase of Cu_xS near stoichiometric composition, at first DFT calculations were performed systematically on different possible stoichiometric Cu_2S crystal structures. The possible set of structures chosen for this study were antifluorite- (AF-) Cu_2S, acanthite like, berzelianite-like, stromeyerite-like structures, and other structures provided by material project database [28]. In addition, for comparison purposes, known Cu deficient Cu_xS phases have been considered as well in their stoichiometric limit. After these structures were relaxed, we compared their energetics to search for the most favorable Cu_2S structure.

Table 2: Cohesive energies of selected low-energy stoichiometric Cu_2S structures are listed.

Structure name	Cohesive energy per formula unit (eV)
Acanthite	−10.653
Material project	−10.638
Low chalcocite	−10.637
Stromeyerite	−10.631
AF-Cu_2S	−10.379
Berzelianite	−9.995

Then choosing structure with the lowest relaxed energy along with other few possible structures with comparable energies, such as low chalcocite structure, we formed copper vacant $Cu_{1.98}S$ structures and did further calculation on them. In particular, the low chalcocite structure has been considered for comparison because we are interested in Cu_xS compositions near stoichiometric Cu_2S, and low chalcocite structure is known to be the stoichiometric structure at low temperature.

In order to have a better understanding of the electronic properties, systematic analyses of density of states (dos) plots, band structures, and Cu vacancy formation energies have been performed. The defect formation energy of Cu vacancy was obtained using the following equation:

$$E_f = E_{\text{tot}}(D) - E_{\text{tot}}(0) + n\left(\mu_{\text{Cu}} + \Delta\mu_{\text{Cu}}\right), \quad (1)$$

where $E_{\text{tot}}(D)$ is total energy of Cu vacancy containing cell, $E_{\text{tot}}(0)$ is total energy of cell without defect, n is the number of Cu atoms removed from a defect free cell, and μ_{Cu} is the chemical potential of Cu reservoir, which was taken to be the bulk phase of copper. In addition, for the stability of Cu_xS, $\Delta\mu_{\text{Cu}}$ require the following condition to be satisfied:

$$x\Delta\mu_{\text{Cu}} + \Delta\mu_{\text{S}} = \Delta H_{\text{Cu}_x\text{S}}(\text{bulk}), \quad (2)$$

where we have calculated the formation enthalpy or heat of formation [29] of Cu_xS using the definition

$$\Delta H = E\left(\text{Cu}_x\text{S}\right) - xE(\text{Cu}) - E(\text{S}), \quad (3)$$

where ΔH is heat of formation, $E(Cu_xS)$ is the total energy per formula unit, and E(Cu) and E(S) are total energy per Cu atom in bulk phase and per S atom in stable S_8 phase, respectively. The cohesive energies of selected relaxed structures are calculated using the following definition:

$$E_{\text{coh}} = E\left(\text{Cu}_2\text{S}\right) - 2E_{\text{Cu}} - E_{\text{S}}, \quad (4)$$

where E_{Cu} and E_{S} are free atomic energy of copper and sulfur, respectively. A software program called VESTA [30] was used for visualization purposes.

3. Results and Discussions

The cohesive energies of some selected stoichiometric Cu_2S are presented in Table 2. Among these structures, cohesive energy of the acanthite like structure was found to be

Table 3: DFT optimized lattice parameters for $Cu_{1.98}S$ models are listed.

Structure	a (Å)	b (Å)	c (Å)	α(°)	β (°)	γ (°)
Low chalcocite ($Cu_{1.98}S$)	15.01	11.99	13.23	90	116	90
Acanthite like ($Cu_{1.98}S$)	12.07	14.37	13.69	90	89	90

−10.653 eV per formula unit and is the lowest among all structures. In comparison, the cohesive energy of low chalcocite structure is −10.637 eV per formula unit. Note that acanthite is Ag_2S mineral, where for the sake of the present study Ag is replaced by Cu and has been relaxed without any symmetry constrained. The resulting acanthite like structure of Cu_xS was found to be a very robust structure. Another closely related mineral structure stromeyerite, AgCuS, where Ag is replaced by Cu, has cohesive energy of −10.631 eV per formula unit. On the other hand, structure derived from Cu_2Se (berzelianite) by replacing Se by S was not very favorable with cohesive energy of −9.995 eV per formula unit.

From the above discussion it is clear that acanthite like Cu_2S has most favorable structure at the stoichiometric limit as predicted by DFT total energy calculations. Hence, for DFT + U, we have optimized the U values with respect to the acanthite structure. Note that in Cu_2S, Cu has d^{10} band so Cu here has +1 oxidation state (Cu^{1+}). Hence, even though the U value is optimized for acanthite structure, the same value in principle can be applied to other Cu_2S structures as well. We have tested with several values for U on Cu 3d band to calculate the band gap of Cu_2S and compared with the lowest known experimental gap of 1.1 eV [7]. In general, band gap increases with the value of U. However, though for Cu_2S band gap did increase from 0.152 eV value to a value of 0.905 eV with the application of U up to 7 eV, the gap became less sensitive to further increment of U. Such as with U = 9 eV, the band gap becomes 1.090 eV. The reason is the d^{10} nature of the Cu 3d orbital. For higher value of U, the completely filled 3D band goes lower in energy within the valence band, which can only indirectly affect the band gap through S 2p hybridization. Even though U = 9 eV gave band gap value closer to the known experimental range, from U = 7 eV to 9 eV the band gap became indirect to direct. As Cu_2S is experimentally known to be an indirect gap semiconductor [31], U = 7 eV would provide a picture closer to the reality. In addition, our previous study on other Cu^{1+}-compounds showed improved results with similar values of U [32, 33]. Hence, U = 7 eV has been selected for this study as an optimal value.

In fact, at the range of x from 1.96 to up to 2, acanthite like structure was found to be even more favorable than low chalcocite structure in this study. At the stoichiometric limit, although acanthite like Cu_2S was found to be more favorable structure, it is more prone to form Cu vacancies even at Cu rich growth condition (will be discussed in the following). Hence, it is less likely to be stable in pristine form at the stoichiometric compositional limit. Like low chalcocite, acanthite structure is also monoclinic in nature, however with much simpler unit cell of total 12 atoms (8 Cu and 4 S atoms), whereas low chalcocite unit cell has 144 atoms.

In the following, we present results comparing both low chalcocite and acanthite structures. This choice is due to the fact that these two structures are two most favorable structures for Cu_2S from theory point of view. Furthermore as low chalcocite has been experimentally observed, it is important to compare properties of Cu deficient acanthite structure against it. First we created a supercell of acanthite like structure containing 96 Cu atoms and 48 S atoms similar to a low chalcocite unit cell. In order to create a composition Cu_xS with x = 1.98, we created a vacancy in both structures and relaxed them fully using DFT. We present fully optimized DFT lattice parameters for two $Cu_{1.98}S$ structures in Table 3. Acanthite ($Cu_{1.98}S$) structure is slightly larger than low chalcocite ($Cu_{1.98}S$) as volume per formula unit of acanthite ($Cu_{1.98}S$) is 4.73 $Å^3$ higher than the latter. The crystal structure also shows a significant difference between the two structures which can be seen in Figure 1. Acanthite structure remained almost orthorhombic, whereas the monoclinic nature of low chalcocite is evident. In addition, Cu atoms seem to follow a particular layered structure in acanthite like ($Cu_{1.98}S$), in contrast to low chalcocite ($Cu_{1.98}S$) such layer or any Cu ordering that is absent. The average Cu-Cu bond length is very similar, namely, 2.67 Å for acanthite ($Cu_{1.98}S$) and 2.69 Å for low chalcocite ($Cu_{1.98}S$). These calculated Cu-Cu bond lengths are about 5% higher than metallic Cu-Cu distance of 2.55 Å (DFT), indicating some Cu-Cu interaction may be present in both structures. Average Cu-S bond length is 2.33 Å in acanthite ($Cu_{1.98}S$) whereas it is 2.36 Å in low chalcocite ($Cu_{1.98}S$). The smaller Cu-S bond length in acanthite compared to the low chalcocite is due to the almost planer Cu-S layered structure. Note that in acanthite both Cu-Cu and Cu-S average bond lengths are smaller than the low chalcocite structure, even though the volume in acanthite is larger. This is a consequence of the Cu-S and Cu-Cu layered structure in acanthite, where the interlayer separations are larger than these average bonds. It is important to mention here that, as opposed to djurleite or digenite structures, acanthite structure of $Cu_{1.8}S$ cannot be derived from the low chalcocite structure by simply creating vacancies in it. Hence, acanthite and low chalcocite are structurally distinct structures.

In order to find the probability of forming defect structures at composition x = 1.98 we calculated the defect formation energy using (1) at two extreme cases: (i) at Cu-rich (or S-poor) condition where Cu has the total chemical potential equal to its bulk phase and (ii) at Cu-poor (or S-rich) condition, where sulfur is assumed to be in thermal equilibrium with stable S_8 phase (bulk). To form stable bulk Cu_2S the constraint on chemical potentials of Cu and S is given by (2). Figure 2 shows schematically the calculated Cu vacancy formation energy (by (1) and (2)) as a function of

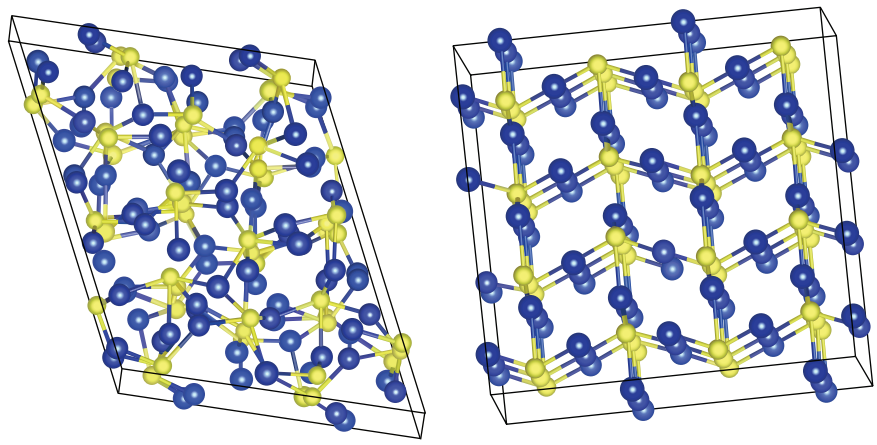

Figure 1: Crystal structures for two lowest-energy $Cu_{1.98}S$ structures are shown here.

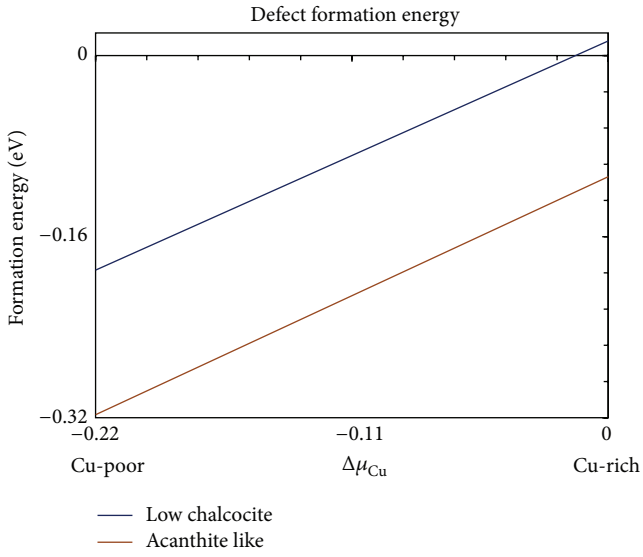

Figure 2: DFT calculated defect formation energy as a function of copper chemical potential.

copper chemical potential for acanthite and low chalcocite structures. This figure reveals two important results: (i) Cu vacancy formation energy for low chalcocite is positive at Cu-rich condition whereas for acanthite structure formation energies are negative at both cases and (ii) at both Cu-rich and Cu-poor conditions, the Cu vacancy formation energy of acanthite structure is lower than that of low chalcocite. These imply that formation of Cu vacancies in acanthite structure ($Cu_{1.98}S$) is thermodynamically more probable than low chalcocite ($Cu_{1.98}S$). In addition, it can be argued from Figure 2 that low chalcocite has a possibility to remain stoichiometric at a Cu rich growth condition. However, acanthite structure would form Cu vacancies spontaneously at any growth condition. Hence, even though acanthite has lower energy (i.e., higher stability) at stoichiometric composition of Cu_2S, low chalcocite is a relatively more probable candidate for pristine stoichiometric Cu_2S. However, it should be noted that at Cu-rich condition, even though formation energy of Cu vacancy is positive for low chalcocite, it is very still very small.

We note that acanthite structure ($Cu_{1.98}S$) has the lowest heat of formation, −0.447 eV per formula unit, whereas for low chalcocite ($Cu_{1.98}S$) it is 27 meV per formula unit higher. Also note that, for pristine Cu_2S, the difference of formation enthalpies between these two structures is 16 meV. On the other hand, heat for formation for acanthite $Cu_{1.98}S$ is lower than that of stoichiometric Cu_2S acanthite, which is evident from the negative formation energies of Figure 2. These indicate that Cu vacancies lower the total energy of acanthite structure even more than that of the low chalcocite structure. Hence, Cu vacancy defect formation energy and heat of formation calculation both suggest that acanthite structure is energetically more favorable as $Cu_{1.98}S$. However, acanthite structure has not been experimentally observed yet. It is possible that around this composition ($x = 1.98$), due to close proximity of energies, at room temperature acanthite structure can simply coexist with low chalcocite, which would make the detection even more complicated.

Next, we present electronic properties of acanthite structure of $Cu_{1.98}S$ at both DFT and DFT + U level of theory where, as mentioned earlier, $U = 7$ eV applied to Cu-d band. The band structure is provided in Figure 3. As expected, without any additional term, DFT underestimates the band gap; in fact in this case the conduction and valence bands overlap implying a metal like behavior. On the other hand, DFT + U opened up the gap; the calculated band gap is about 0.82 eV which is an indirect gap, along Γ to A direction. In contrast, opening of band gap in low chalcocite with DFT + U is smaller; however, the gap was found to be direct. These gaps are still slightly lower than observed experimental band gaps for other Cu_xS which may be due to DFT related limitations.

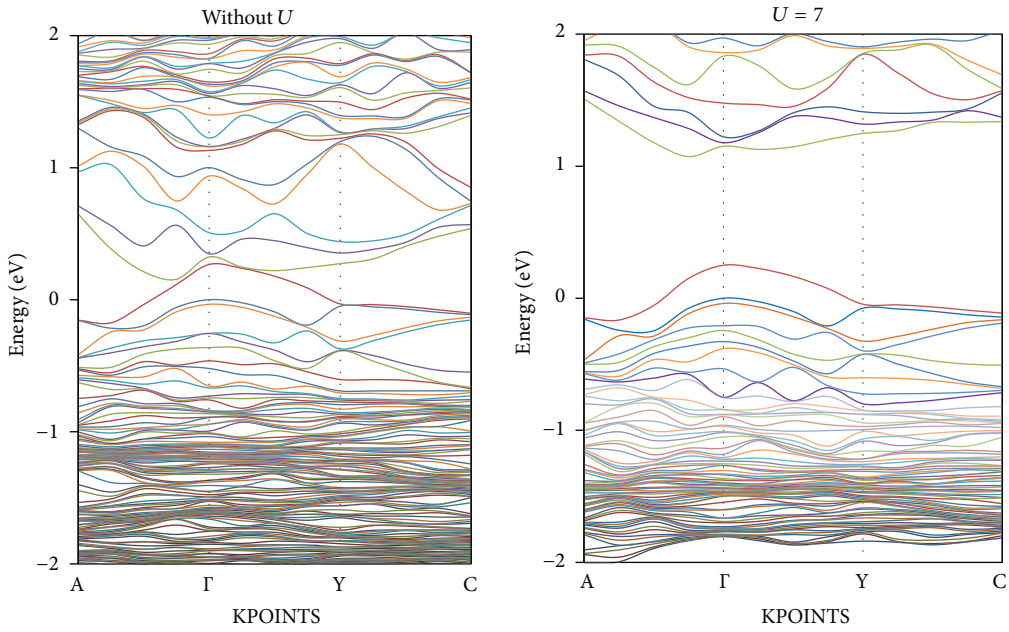

Figure 3: Band Structures for acanthite like structure ($Cu_{1.98}S$) with DFT and DFT + U theories.

The top of the valence band for both structures is unoccupied which indicate a p-type doping scenario, as expected due to Cu vacancy.

The total density of states (DOS) and partial density of states (pDOS) calculated using DFT and DFT + U are provided in Figure 4. In these plots the highest occupied band energy is scaled to 0 eV. A small peak around 0 eV is due to the presence of a hole state created by Cu vacancy. Here, it is important to provide rationale for the application of DFT + U to open band gap compared to DFT. In pristine Cu_2S, Cu 3D bands are expected to be fully occupied ($3d^{10}$); hence the application of U to such fully occupied band cannot open up a gap between occupied and unoccupied 3D band as a direct consequence as discussed earlier; rather it changes the energy of 3d band's position and increases its localization. Application of U in such case changes the hybridization of Cu 3d band with other bands, and hence given favorable condition can open up a band gap. We see a prominent peak at around −13.8 eV (DFT) and −13.1 eV (DFT + U) which is mainly due to low lying S s-band (not shown in pDOS). This shift is due to the change in hybridization as the Cu-d band became more localized with the application if U potential. This can be justified by the fact that the width of the valence band has been reduced by 0.9 eV due to the application of DFT + U. Such results clearly indicate the localization effect of Cu-d electrons in $Cu_{1.98}S$. As the Cu-d band lowers in energy compared to the scenario where U was not applied, the top of the valence band is no longer dominated by Cu-d. As an additional effect, lowering of 3D band's energy also lowers the valence band maximum (VBM), even though the feature of the top three bands remained almost the same as seen in Figure 3. Hence an increasing value of U lowers the position of VBM as well. The p-dos plots show that there is more dominance of S-p-band at conduction bands especially after including the correlation term. The latter seems more realistic as Cu-d-band being fully occupied has no empty band for electrons. The presence of Cu-d-band and S-p-band at the valence band and conduction band is suitable for p-d optical transition which is beneficial from photoconductivity point of view.

4. Conclusions

In conclusion, a new phase of copper sulfide (Cu_xS) at composition around $x = 1.98$ using density functional theory and crystal database has been proposed. The calculated formation energies and heat of formation indicated that acanthite like structure as a phase can occur as $Cu_{1.98}S$. Interestingly, acanthite ($Cu_{1.98}S$) is found to be structurally more preferable and thermodynamically more stable than low chalcocite structure even at the stoichiometric limit of Cu_2S. In addition, acanthite structure is more prone to Cu vacancy formation than low chalcocite. It is possible that near stoichiometric composition ($x \rightarrow 2$) of Cu_xS, both acanthite like and low chalcocite structures can coexist. For $Cu_{1.98}S$, Cu-S forms a simple layer like structure with higher cell volume than the corresponding low chalcocite structure. However, both the nearest Cu-Cu and Cu-S average distances are lower in acanthite than in low chalcocite. Overall, the electronic structure near valence band is found to be similar to that of low chalcocite, though the valence band maximum of acanthite is higher in energy. Our results will provide an important insight into the complex nature of the Cu_xS phase space.

Conflict of Interests

The authors declare that there is no conflict of interests regarding the publication of this paper.

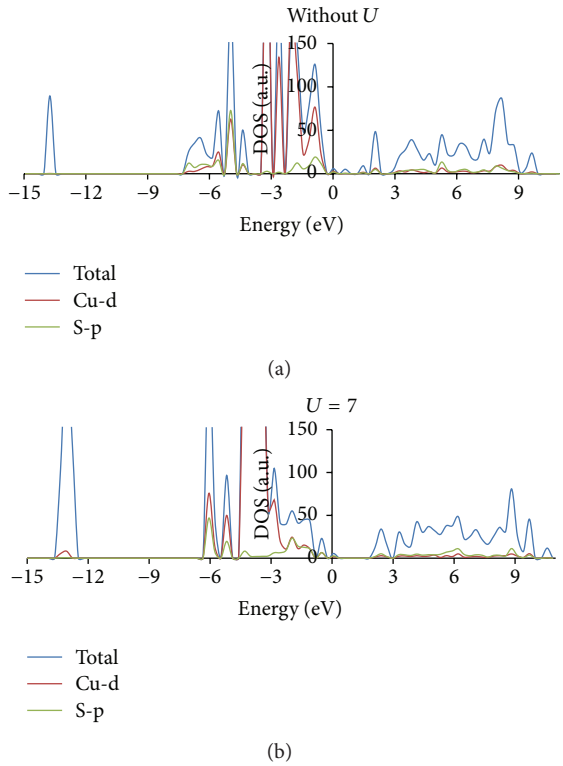

FIGURE 4: Dos plots for acanthite like structure ($Cu_{1.98}S$) are shown. The top panel is for DFT calculation and the bottom one is for DFT + U. Cu-d and S-p dos are zoomed (100x) to have better resolution.

Acknowledgments

The authors are grateful to National Renewable Energy Laboratory for funding (Subcontract no. XEJ-3-23232-01). Computations were performed at the University of Texas at Arlington's High Performance Computing Center (HPC) and at the Computing System of Texas Advanced Computing Center (TACC), Austin.

References

[1] B. G. Caswell, G. J. Russell, and J. Woods, "Photoconductive effects in CdS-Cu_2S photovoltaic cells," *Journal of Physics D: Applied Physics*, vol. 8, no. 15, pp. 1889–1900, 1975.

[2] L. L. Kazmerski, F. R. White, and G. K. Morgan, "Thin-film $CuInSe_2$/CdS heterojunction solar cells," *Applied Physics Letters*, vol. 29, no. 4, p. 268, 1976.

[3] J. A. Bragagnolo, A. M. Barnett, J. E. Phillips, R. B. Hall, A. Rothwarf, and J. D. Meakin, "The design and fabrication of thin-film CdS/Cu2S cells of 9.15-percent conversion efficiency," *IEEE Transactions on Electron Devices*, vol. 27, no. 4, pp. 645–650, 1980.

[4] W. D. Gill and R. H. Bube, "Photovoltaic properties of Cu2S-CdS heterojunctions," *Journal of Applied Physics*, vol. 41, no. 9, pp. 3731–3738, 1970.

[5] R. W. Potter, "An electrochemical investigation of the system copper-sulfur," *Economic Geology*, vol. 72, no. 8, p. 1524, 1977.

[6] H. T. Evans Jr., "The crystal structures of low chalcocite and djurleite," *Zeitschrift für Kristallographie*, vol. 150, pp. 299–320, 1979.

[7] P. Lukashev, W. Lambrecht, T. Kotani, and M. van Schilfgaarde, "Electronic and crystal structure of $Cu_{2-x}S$: full-potential electronic structure calculations," *Physical Review B*, vol. 76, no. 19, Article ID 195202, 2007.

[8] Q. Xu, B. Huang, Y. Zhao, Y. Yan, R. Noufi, and S. Wei, "Crystal and electronic structures of Cu_xS solar cell absorbers," *Applied Physics Letters*, vol. 100, no. 6, Article ID 061906, 2012.

[9] A. M. Al-Dhafiri, G. J. Russell, and J. Woods, "Degradation in CdS-Cu_2S photovoltaic cells," *Semiconductor Science and Technology*, vol. 7, no. 8, pp. 1052–1057, 1992.

[10] P. Kumar, R. Nagarajana, and R. Sarangi, "Quantitative X-ray absorption and emission spectroscopies: electronic structure elucidation of Cu_2S and CuS," *Journal of Materials Chemistry C*, vol. 1, no. 13, pp. 2448–2454, 2013.

[11] M. Lotfipour, T. Machani, D. P. Rossi, and K. E. Plass, "Alpha-chalcocite nanoparticle synthesis and stability," *Chemistry of Materials*, vol. 23, no. 12, pp. 3032–3038, 2011.

[12] T. Machani, D. P. Rossi, B. J. Golden, E. C. Jones, M. Lotfipour, and K. E. Plass, "Synthesis of monoclinic and tetragonal chalcocite nanoparticles by iron-induced stabilization," *Chemistry of Materials*, vol. 23, no. 24, pp. 5491–5495, 2011.

[13] S. C. Riha, S. Jin, S. V. Baryshev, E. Thimsen, G. P. Wiederrecht, and A. B. F. Martinson, "Stabilizing Cu_2S for photovoltaics one atomic layer at a time," *ACS Applied Materials & Interfaces*, vol. 5, no. 20, pp. 10302–10309, 2013.

[14] E. Hirahara, "The physical properties of cuprous sulfides semiconductors," *Journal of the Physical Society of Japan*, vol. 6, no. 6, pp. 422–427, 1951.

[15] L.-W. Wang, "High chalcocite Cu_2 S: a solid-liquid hybrid phase," *Physical Review Letters*, vol. 108, Article ID 085703, 2012.

[16] B. J. Wuensch and M. J. Buerger, "The crystal structure of chalcocite, Cu_2S," *Mineralogical Society of America—Special Papers*, vol. 1, pp. 164–170, 1963.

[17] M. J. Buerger and B. J. Wuensch, "Distribution of atoms in high chalcocite, Cu_2S," *Science*, vol. 141, no. 3577, pp. 276–277, 1963.

[18] S. Djurle, "An X-ray study on the system Cu-S," *Acta Chemica Scandinavica*, vol. 12, pp. 1415–1426, 1958.

[19] G. Will, E. Hinze, and A. R. M. Abdelrahman, "Crystal structure analysis and refinement of digenite, Cu1.8S, in the temperature range 20 to 500°C under controlled sulfur partial pressure," *European Journal of Mineralogy*, vol. 14, no. 3, pp. 591–598, 2002.

[20] K. Koto and N. Morimoto, "The crystal structure of anilite," *Acta Crystallographica Section B*, vol. 26, no. 7, pp. 915–924, 1970.

[21] G. Kresse and J. Furthmüller, "Efficient iterative schemes for ab initio total-energy calculations using a plane-wave basis set," *Physical Review B*, vol. 54, no. 16, pp. 11169–11186, 1996.

[22] G. Kresse and J. Furthmüller, "Efficiency of ab-initio total energy calculations for metals and semiconductors using a plane-wave basis set," *Computational Materials Science*, vol. 6, no. 1, pp. 15–50, 1996.

[23] J. P. Perdew, K. Burke, and M. Ernzerhof, "Generalized gradient approximation made simple," *Physical Review Letters*, vol. 77, no. 18, pp. 3865–3868, 1996.

[24] P. E. Blöchl, "Projector augmented-wave method," *Physical Review B*, vol. 50, no. 24, pp. 17953–17979, 1994.

[25] M. Gajdoscaron, K. Hummer, G. Kresse, J. Furthmuller, and F. Bechstedt, "Linear optical properties in the projector-augmented wave methodology," *Physical Review B*, vol. 73, no. 4, Article ID 045112, 9 pages, 2006.

[26] V. I. Anisimov, J. Zaanen, and O. K. Andersen, "Band theory and Mott insulators: Hubbard U instead of Stoner I," *Physical Review B*, vol. 44, no. 3, pp. 943–954, 1991.

[27] S. L. Dudarev, G. A. Botton, S. Y. Savrasov, C. J. Humphreys, and A. P. Sutton, "Electron-energy-loss spectra and the structural stability of nickel oxide: an LSDA+U study," *Physical Review B: Condensed Matter and Materials Physics*, vol. 57, no. 3, pp. 1505–1509, 1998.

[28] A. Jain, S. P. Ong, G. Hautier et al., "Commentary: the materials project: a materials genome approach to accelerating materials innovation," *APL Materials*, vol. 1, no. 1, Article ID 011002, 2013.

[29] L. A. Curtiss, K. Raghavachari, P. C. Redfern, and J. A. Pople, "Assessment of Gaussian-2 and density functional theories for the computation of enthalpies of formation," *Journal of Chemical Physics*, vol. 106, no. 3, pp. 1063–1079, 1997.

[30] K. Momma and F. Izumi, *VESTA: A Three-Dimensional Visualization System*, 2011.

[31] G. Liu, T. Schulmeyer, J. Brötz, A. Klein, and W. Jaegermann, "Interface properties and band alignment of Cu_2S/CdS thin film solar cells," *Thin Solid Films*, vol. 431-432, pp. 477–482, 2003.

[32] P. Sarker, D. Prasher, N. Gaillard, and M. N. Huda, "Predicting a new photocatalyst and its electronic properties by density functional theory," *Journal of Applied Physics*, vol. 114, no. 13, Article ID 133508, 2013.

[33] M. N. Huda, Y. Yan, A. Walsh, S.-H. Wei, and M. M. Al-Jassim, "Group-IIIA versus IIIB delafossites: electronic structure study," *Physical Review B*, vol. 80, Article ID 035205, 2009.

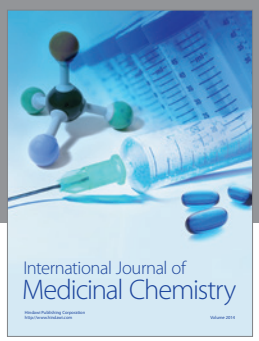

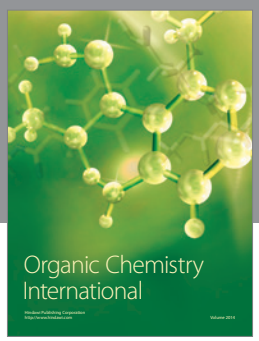

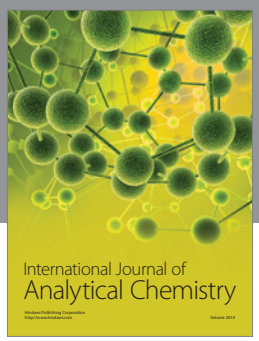

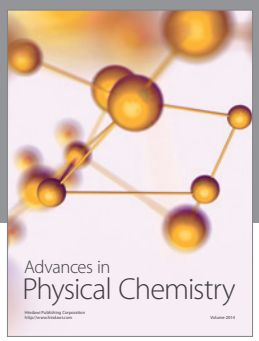

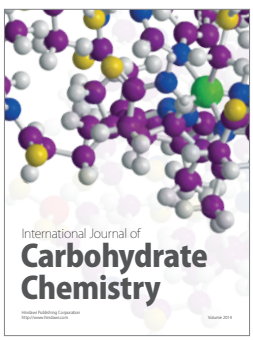

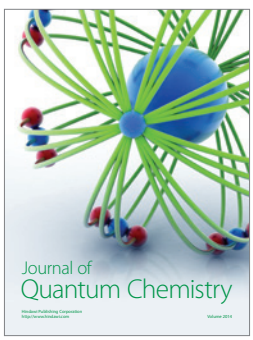

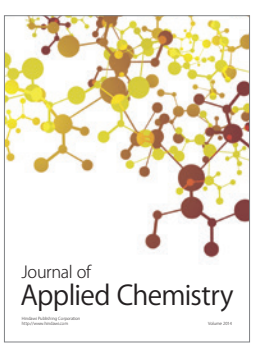

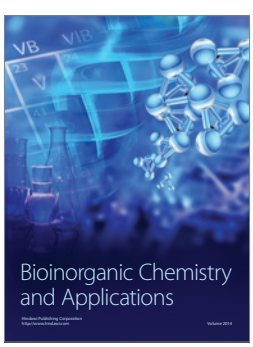

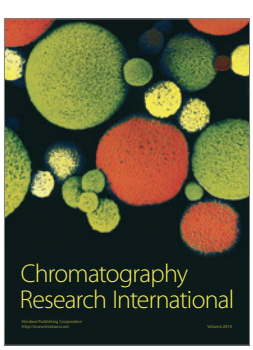

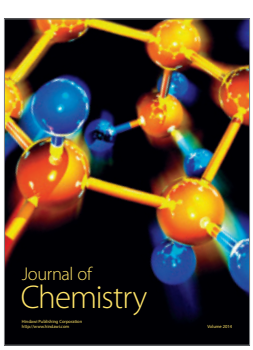

Hindawi

Submit your manuscripts at
http://www.hindawi.com